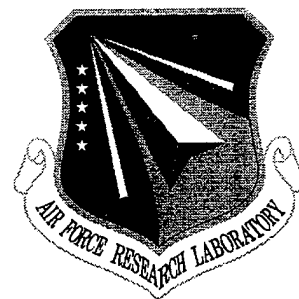


AFRL-SN-RS-TR-1998-24
Final Technical Report
February 1998



POTENTIALITIES OF COHERENT SYSTEMS IN RF PHOTONICS

Optivision, Inc.

Robert T. Weverka

APPROVED FOR PUBLIC RELEASE; DISTRIBUTION UNLIMITED.

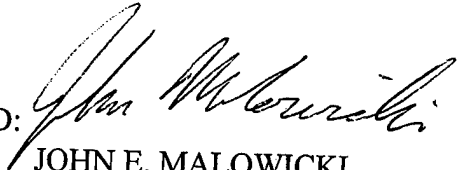
19980324 015

19980324 015

AIR FORCE RESEARCH LABORATORY
SENSORS DIRECTORATE
ROME RESEARCH SITE
ROME, NEW YORK

AFRL-SN-RS-TR-1998-24 has been reviewed and is approved for publication.

APPROVED:



JOHN E. MALOWICKI
Project Engineer

FOR THE DIRECTOR:



ROBERT G. POLCE, Acting Chief
Rome Operations Office
Sensors Directorate

DESTRUCTION NOTICE - For classified documents, follow the procedures in DOD 5200.22M, Industrial Security Manual or DOD 5200.1-R, Information Security Program Regulation. For unclassified limited documents, destroy by any method that will prevent disclosure of contents or reconstruction of the document.

If your address has changed or if you wish to be removed from the Air Force Research Laboratory Rome Research Site mailing list, or if the addressee is no longer employed by your organization, please notify Air Force Research Laboratory/SNDP, 25 Electronic Pky, Rome, NY 13441-4514. This will assist us in maintaining a current mailing list.

Do not return copies of this report unless contractual obligations or notices on a specific document require that it be returned.

REPORT DOCUMENTATION PAGE

Form Approved
OMB No. 0704-0188

Public reporting burden for this collection of information is estimated to average 1 hour per response, including the time for reviewing instructions, searching existing data sources, gathering and maintaining the data needed, and completing and reviewing the collection of information. Send comments regarding this burden estimate or any other aspect of this collection of information, including suggestions for reducing this burden, to Washington Headquarters Services, Directorate for Information Operations and Reports, 1215 Jefferson Davis Highway, Suite 1204, Arlington, VA 22202-4302, and to the Office of Management and Budget, Paperwork Reduction Project (0704-0188), Washington, DC 20503.

1. AGENCY USE ONLY (Leave blank)	2. REPORT DATE February 1998	3. REPORT TYPE AND DATES COVERED FINAL Apr 97 - Jul 97	
4. TITLE AND SUBTITLE POTENTIALITIES OF COHERENT SYSTEMS IN RF PHOTONICS		5. FUNDING NUMBERS C - F30602-97-C-0108 PE - 62702F PR - 4600 TA - P6 WU - PG	
6. AUTHOR(S) Robert T. Weverka		8. PERFORMING ORGANIZATION REPORT NUMBER	
7. PERFORMING ORGANIZATION NAME(S) AND ADDRESS(ES) Optivision, Inc. 3450 Hillview Ave Palo Alto CA 94304		10. SPONSORING / MONITORING AGENCY REPORT NUMBER AFRL-SN-RS-TR-1998-24	
9. SPONSORING / MONITORING AGENCY NAME(S) AND ADDRESS(ES) Air Force Research Laboratory/SNDP 25 Electronic Pky Rome NY 13441-4515		11. SUPPLEMENTARY NOTES Air Force Research Laboratory Project Engineer: John E. Malowicki, SNDP, (315) 330-4682	
12a. DISTRIBUTION AVAILABILITY STATEMENT APPROVED FOR PUBLIC RELEASE; DISTRIBUTION UNLIMITED		12b. DISTRIBUTION CODE	
13. ABSTRACT (Maximum 200 words) Mutually coherent RF photonic remoting is compared with mutually incoherent RF photonic systems. Current multi-channel RF photonic systems for phased array antennas are implemented with mutually incoherent sources. Additional photonic processing operations with these systems cannot take advantage of coherent fan-in gain and suffer the DC bias build up well known in incoherent optical signal processing. Mutually coherent RF photonic systems are investigated and shown to have higher gain and higher dynamic range than incoherent systems. The trade-off between subarray partitioning size and link dynamic range is also studied.			
14. SUBJECT TERMS mutually coherent/incoherent RF photonics, phased arrays, photodetectors, shot noise, thermal noise, modulators		15. NUMBER OF PAGES 28	
17. SECURITY CLASSIFICATION OF REPORT UNCLASSIFIED		16. PRICE CODE	
18. SECURITY CLASSIFICATION OF THIS PAGE UNCLASSIFIED		20. LIMITATION OF ABSTRACT UL	
19. SECURITY CLASSIFICATION OF ABSTRACT UNCLASSIFIED		20. LIMITATION OF ABSTRACT	

Table of Contents

Table of Contents	i
List of Figures	ii
Executive Summary	iii
1. Introduction	1
2.0 Technical Results	2
2.1 Task 1 System Impacts of Coherent RF Photonics	2
System Analysis	2
2.2 Task 2 Impact of RF Photonic processing on component requirements	8
2.3 Task 3 Optimum Subarray Partitioning	14
2.4 Task A DTIC Search	16
3.0 References	17

List of Figures

Figure 1 “Incoherent and coherent systems for performance comparison”	3
Figure 2 “Microwave power addition”	5
Figure 3 “Detector structures for high power microwave signal detection”	10
Figure 4 “Link with detector from Figure 3c”	11
Figure 5 “Frequency-wavenumber space representation of the received signals”	15

Executive Summary

The principal goal of the effort reported here was to compare mutually coherent RF photonic remoting with mutually incoherent RF photonic systems. Current multi-channel RF photonic systems for phased array antennas are implemented with mutually incoherent sources¹. Additional photonic processing operations with these systems cannot take advantage of coherent fan-in gain and suffer the DC bias build up well known in incoherent optical signal processing². We have investigated mutually coherent RF photonic systems and shown how these systems will have higher gain and higher dynamic range than incoherent systems.

RF photonic component development is currently driven by link requirements, where a link consists of electrooptic signal conversion, transmission with possible variable delay, and optoelectronic signal conversion³. When the RF photonic signals are used in coherent systems before detection, the component specifications are subject to a different set of trade-offs. We have analyzed the requirements of RF photonic components optimized for coherent RF photonic systems.

Current partitioning of phased arrays into electronic phase-steered subarrays feeding optical true-time-delay arrays is driven by beam squint requirements. We have studied the dynamic range impact of an increasing number of optical links (smaller subarrays) and shown a structure in which there is little cost and large advantages.

The key results of this investigation is that with coherent systems a finite optical power is sufficient to remote an arbitrarily large array. Incoherent systems require optical power to grow in proportion to array size, and hence that part of the optical system has a finite cost per antenna element. For coherent systems, this new result tells us that a finite power optical source can be spread over an arbitrarily large number of photonic links, an consequently the cost of the light source per antenna element falls with the size of the array. Additionally, a single detector array structure which does not grow with array size is all that is needed.

For a coherent system with no preamplifiers in front of the optical modulators, the total optical power required is 10 Watts, regardless of array size. This optical power level will provide the entire array with low noise figure transmission of the optical signals.

1. Introduction

Emerging DoD missions require broadband phased array antennas for radar, communications, and electronic warfare (EW) applications. Programs in the development of phased array antenna systems are targeted at increasing the performance of phased array antennas while decreasing their size, weight, radar cross-section and cost, and increasing their reliability. Performance goals of current phased array antenna programs include increased dynamic range, higher frequency operation, increased bandwidth, larger numbers of antenna elements, apertures shared by multiple operating bands, and improved precision in beam steering and null steering. Broadband phased arrays require the use of true-time-delay beam steering, and have very large processing throughput requirements. The advantages of photonics for providing true-time-delay in phased array systems is well-known.

It is now widely recognized that optics provides an ideal technology for implementing true-time-delays in phased array antennas¹. There have been impressive field demonstrations of the use of fiber-optics in true-time-delay beam steering subsystems. Here we examine the system dynamic range improvements resulting from a coherent beam former.

Two emerging component level developments which enable high dynamic range coherent photonic systems are (1) the advent of high power linear photodetectors, and (2) means of correcting phase changes of photonic carriers in the presence of vibrations and thermal fluctuations in the transmission fiber. These developments allow us to use coherent optical systems in place of the current systems which use incoherent optics. Our results require the use of high power photodetectors. We propose an easily realizable alternative to current investigations in high power photodetectors, and analyze the system impact of these developments.

Subarray implementations of true-time-delay (TTD) photonic beam steering require higher dynamic range in each of the links carrying the subarray data. This leads to higher component costs in the photonic links. Smaller subarrays require a larger number of optoelectronic links for the entire array. We show how the coherent system largely circumvents this trade-off by because its laser and photodetector requirements are independent of the number of array elements.

2.0 Technical Results

2.1 Task 1 System Impacts of Coherent RF Photonics

In many systems under development RF photonics is being used to remote each of the antenna elements of a phased array independently. For such systems there is no difference between mutually coherent and mutually incoherent light beams used to remote the array. In these systems the signals from a phased array are weighted and summed to form the output *after detection*. As we develop systems which utilize more RF photonic processing for more of the functions, the weighted summation used to form the antenna beam will be done optically. Whether this sum is done coherently or incoherently has great impact on the system performance and component and link requirements. In this task we have explored the impacts of using coherent RF photonic systems for phased array radar.

Coherent RF photonic systems have the potential to provide increased gain and improved dynamic range in phased array antennas. This advantage is provided by coherent fan-in gain. Optical coherent fan-in gain is gain over and above the normal phased array antenna gain provided by summing the signals from the elements of the phased array.

System Analysis

The comparison of incoherent versus coherent phased array antenna systems utilizes the block diagrams shown in Figure 1. Both the coherent and incoherent systems use the same total optical power P_0 . The incoherent system of Figure 1a uses a variable time delay unit on each of the channels and the optical power is converted to electrical current by the photodetector before summing to form the antenna main beam. The coherent system of Figure 1b uses the same variable time delay unit on each of the channels. The output of the variable time delay units is corrected for the optical phase variations and combined optically before photodetection to form the antenna main beam output. In the next two sections we analyze the incoherent and the coherent system.

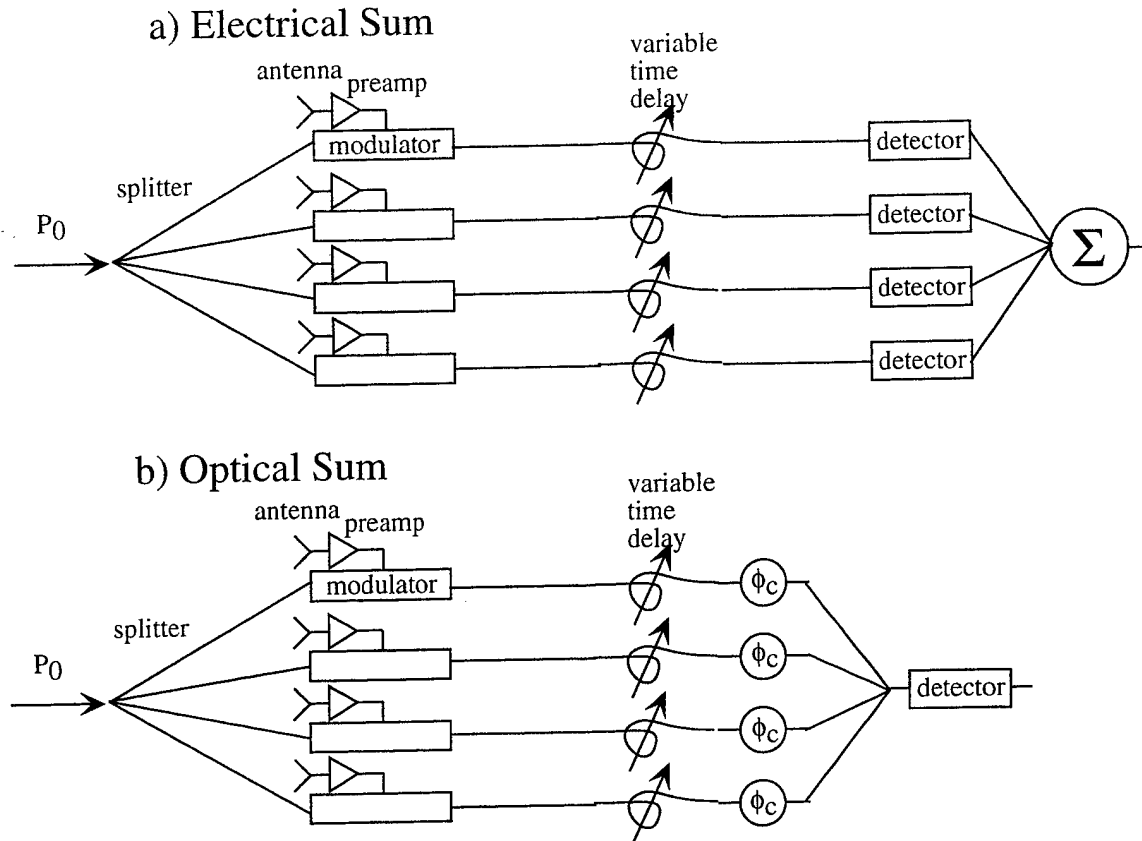


Figure 1. Incoherent and coherent systems for performance comparison. Figure 1a shows the incoherent system with the optical modulators followed by time delay units and optical detectors. Figure 1b shows the coherent system where we have replaced the detectors with phase adjusters and a single detector acting on the combined optical field.

Without loss of generality we use the example of the interferometric intensity modulation for the optical modulator. The amplitude transfer function of the n th device is $(i + \exp[i\phi_n(t)])/2$, where we have assumed the modulator is biased in quadrature and the phase modulation is given by $\phi_n(t) = \pi V_n(t)/V_\pi$, where V_π is the half wave voltage. The total optical power, P_0 , oscillating at the optical frequency ω , is divided N ways to give the output of the n th modulator as

$$a_n(t) = \sqrt{\frac{P_0}{N}} \exp[i\omega t - \phi_m] (i + \exp[i\phi_n(t)])/2 \quad (1)$$

In equation (1) we have assumed the path from the splitter in Figure 1 to each of the modulators has a phase error ϕ_m . For a signal incident on the antenna from the far field, the inputs are related by

$$\phi_n(t) = \phi(t + n a \sin(\theta_s)/c) \quad (2)$$

where a is the array element spacing, θ_s is the angle of incidence of the signal and c is the speed of light. The signals are given the opposite delay, $-na \sin(\theta_s)/c$, by the variable TTD to steer the main beam towards θ_s . Substituting (2) into (1) and including the TTD delay we have

$$a_n(t - na \sin(\theta_s)/c) = \sqrt{\frac{P_0}{N}} \exp[i\omega_l(t - na \sin(\theta_s)/c) - \phi_m] (i + \exp[i\phi(t)])/2 \quad (3)$$

Incoherent System Analysis

Both the coherent and the incoherent system are the same up to this point. In the incoherent system of Figure 1a this signal is intensity detected giving the photocurrent

$$I_n = \Re a_n(t - na \sin(\theta_s)/c) a_n^*(t - na \sin(\theta_s)/c) = \Re \frac{P_0}{2N} (1 + \sin[\phi(t)]) \quad (4)$$

where \Re is the detector responsivity. The bias current generates shot noise and RIN noise from the laser. Additionally there is thermal noise generated at the photodetector output and amplified thermal noise from the modulator input. This gives us the noise

$$N_n = \Re \frac{P_0}{N} eBR_{out} + \left(\Re \frac{P_0}{N} \right)^2 \tau_l BR_{out} + kTB + \Re^2 \frac{P_0^2}{4N^2 V_\pi^2} \pi^2 kTB R_{in} R_{out} \quad (5)$$

where R_{out} is the detector output impedance, e is the electron charge, B is the bandwidth, τ_l is the laser RIN power spectral density, k is Boltzmann's constant, T is temperature, and R_{in} is the modulator input impedance. The signal at each detector output is

$$S_n = \left[\Re \frac{P_0}{2N} \sin[\phi(t)] \right]^2 R_{out} \approx \left[\Re \frac{P_0}{2N} \phi(t) \right]^2 R_{out} \quad (6)$$

The signal and noise terms of equations (5) and (6) are added either in a power sum or a current sum. Both of these kinds of addition give the same signal to noise ratio. We treat here only the power sum version. A passive structure for summing microwave power is shown in Figure 2. The signals at the two outputs of each 4 port 0° hybrid are the sum and difference of the two inputs. Independent noise at the inputs passes equally to each output. Identical signal present at the inputs add in phase at the upper port and cancel at the lower port, thus the hybrid passes all of the power of these signals to the single upper port.

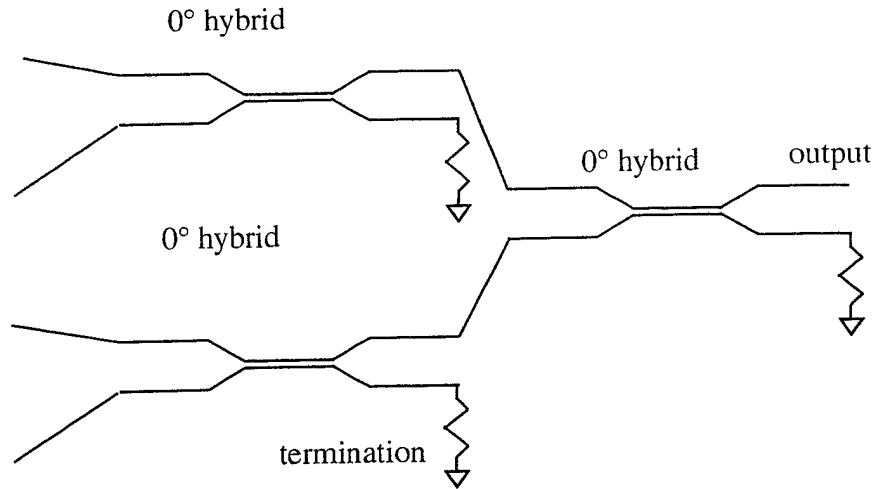


Figure 2. Microwave power addition. The 4 port 0° hybrids provide the sum and difference of the two input signals at the output ports.

Each of the signal terms are in phase due to our TTD giving us a power gain of N in the output. The output of the final summing node of Figure 1 is

$$S = \sum_n^N S_n = \Re^2 \frac{P_0^2}{4N} \frac{\pi^2 V_m^2(t)}{V_\pi^2} R \quad (7)$$

The noise terms due to shot noise and thermal noise are uncorrelated between detectors, so the power passes equally to each hybrid output port. The RIN noise is added with the time delays in the TTD structure. These delays make this RIN noise term add coherently for frequencies lower than the reciprocal of the differential time delay between different channels in the phased array structure and incoherently for larger frequencies. The Noise at the output port is thus

$$Noise = \sum_n^N \langle N_n \rangle = \Re \frac{P_0}{N} eBR + \frac{\Re^2 P_0^2}{N^2} \tau_i BR \Gamma(\theta_s) + kTB + \Re^2 \frac{P_0^2}{4N^2 V_\pi^2} \pi^2 kTB R_m R \quad (8)$$

where we have introduced a correlated power factor addition for the noise terms defined by

$$\Gamma(\theta_s) \equiv \frac{1}{N} \sum_{m,n}^N \Gamma(c/m a \sin(\theta_s) - c/n a \sin(\theta_s)) \quad (9)$$

$\Gamma(\theta_s)$ is between 1 and N depending on the time delay, and had we used independent laser sources to drive the links, we would have $\Gamma(\theta_s) = 1$.

Equations (7) and (8) are our main result for incoherent systems. The gain factor of N in equation (7) over equation (6) is the conventional array gain. For antenna systems, we must use a preamplifier to make the input thermal noise (the last term in eqn (8) dominate.

For a limited optical power, we must increase the preamplifier gain as we go to larger antenna arrays.

Coherent System Analysis

The analysis of the coherent system starts with equation (3). The phase correction and signal combining may be done with a real time hologram or conventional adaptive optical system. The phase of the signals in equation (3) are combined with a common reference $r \exp[i\omega_r t]$, and the low pass filtered version of the intensity is measured to compare the phases. The hologram records the interference between the carrier in equation (3) and the reference. The sideband frequency is beyond the bandwidth to which the low speed phase correction element responds. The hologram thus records the channel number dependent phasor $\exp[i(na \sin(\theta_s)/c) + i\phi_m]$ and upon readout this phase correction gives us the true time delayed version

$$\begin{aligned} a(t) &= \sum_n^N \frac{1}{\sqrt{N}} a_n(t - na \sin(\theta_s)/c) e^{i(na \sin(\theta_s)/c) + i\phi_m} \\ &= \sum_n^N \frac{1}{N} \sqrt{P_0} \exp[i\omega_r t] (i + \exp[i\phi(t)]) / 2 \end{aligned} \quad (10)$$

The first line of equation 10 includes a $1/\text{Sqrt}[N]$. This is the action of an N-way beamsplitter/beamcombiner.

To satisfy the constant radiance theorem, an N-way beamsplitter must have N output ports as well as N input ports. The Power (P) from each of the input ports is divided equally among all N output ports. Consequently, the amplitude into one port is divided by $1/\text{Sqrt}[N]$ at each of the output ports.

Reduced to a regular 2-port beam splitter, we have that the amplitude from each input shows up at the output reduced by $1/\text{Sqrt}[2]$ which is the usual result.

The photocurrent due to the signal of equation 10 is given by

$$I = \Re a(t) a^*(t) = \Re P_0 \left(\frac{1}{2} + \frac{1}{2} \sin[\phi(t)] \right) \quad (11)$$

The bias current generates shot noise and RIN noise from the laser. Additionally there is thermal noise generated at the photodetector output and amplified thermal noise from the modulator input. This gives us the noise

$$\text{Noise} = \Re P_0 e BR + \left(\Re \frac{P_0}{2} \right)^2 \tau_i BR \Gamma(\theta_s) + kTB + \Re^2 \frac{P_0^2}{4NV_\pi^2} \pi^2 kTB R_m R \quad (12)$$

The signal is

$$S = \left[\Re \frac{P_0}{2} \sin[\phi(t)] \right]^2 R \approx \Re^2 \frac{P_0^2}{4} \frac{\pi^2 V_m^2(t)}{V_\pi^2} R \quad (13)$$

comparison of equation (7) with equation (12) shows that the coherent system has N -fold higher gain for the same optical power. In the limit where the last noise terms dominate, both these systems give the normal antenna gain in signal to noise ratio of

$$SNR = \frac{NV_m^2(t)}{kTBR_m} \quad (14)$$

The normal phased array antenna gain is provided by the summation of signal amplitudes from each of the outputs of the phased array elements. After adjusting the phase or time delay of element output, the coherent sum of the amplitudes gives a signal amplitude gain of N for N antenna elements. The thermal noise in each antenna element is independent, and consequently the noise grows as \sqrt{N} . If these signals are represented by optical power (proportional to antenna signal amplitude) the optical summation is the same as electrical summation. The representation of antenna signal amplitude by optical power seems natural at first, since the photodetectors convert optical power into current. If the signals are represented by optical amplitude instead of power, adding the optical amplitudes before converting to photocurrent gives us the N -fold gain in optical amplitude. On squaring this amplitude to get photocurrent we achieve a gain of N^2 . This excess gain may not be used to improve antenna gain over the fundamental N -fold gain of an N element phased array, however it can be used to improve the gain of the underlying RF photonic link. Since typical links have loss and require preamplifiers, this additional gain due to using coherent systems may be utilized to reduce the demands on the preamplifier. Furthermore, with the additional gain the same RF photonic link improves SNR by increasing signal gain prior to addition of the dominant noise term at the detector. This allows the RF photonic links to have higher dynamic range by a factor of $N^{2/3}$.

The increased dynamic range is a direct result of the increased gain of the coherent system. The input modulators have the same ratio of fundamental to two-tone third order products. Since these are given increased gain by a factor of N , they increase the output over the additive noise terms of the link by N . For two-tone third order intermodulation this leads to $N^{2/3}$ increased dynamic range in systems which are limited by additive link noise.

2.2 Task 2 Impact of RF Photonic processing on component requirements

The major impacts of system architecture on component requirements are the impacts on the detector and the modulator. Coherent and incoherent systems both require high power, low noise laser sources. However the analysis compares these two systems given the same available laser power. The best low noise laser sources are expensive and we expect that the best systems will thus use one high power laser source with that power divided over the optical links as shown in task 1.

For this results of task 1 to hold, the system must not be limited by photodetector power. In task 2.2.1 we explore the photodetector structures which allow this. In task 2.2.2 we explore modulator development and the impact of coherent systems on modulator requirements, showing that the modulator sensitivity is reduced in these systems.

Task 2.2.1 Photodetectors

Some of the results of this investigation are predicated on the system not being limited by the power handling capability of the photodetector. There is currently a great deal of research effort in making high speed detectors which can handle a large current. This improvement in photodetectors allows RF photonic systems to be built with high gain, but it is not necessary for low noise figure systems. The antenna applications of RF photonics require good noise figures, not high gain. It is much easier to build photodetectors which satisfy this requirement.

High power handling requires large area on the photodetector, however large area detectors have too high a capacitance to drive 50 Ω at high bandwidth. Figure 3 shows connection schemes for using a large number of small detectors to achieve low capacitance while achieving large total area and thus high saturation power. Figure 3a has the detectors connected in parallel. This configuration is the same as one large detector. The capacitances add and the structure is unsuitable for high frequency operation. Figure 3b shows the detectors combined in a transmission line. The capacitance of the detector is balanced by the inductance of the line between photodetectors in a traveling wave line. This structure adds the currents of the input detectors and has the potential for high speed and high power. This kind of structure is being investigated by a number of researchers to improve detector technology.

The traveling wave structure of Figure 3b has a number of limitations that prevent it from handling arbitrarily large photocurrent. Chief among them is the interaction of the signal current from one detector on the subsequent detectors in the line. The current

flowing in the line introduces a small modulation on the effective bias voltage of the photodetector. This modulation interacts with the photo-generated signal to produce intermodulation terms. At high signal levels, these intermodulation terms can exceed the noise level.

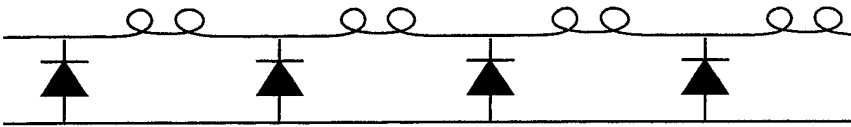
Figure 3c shows an alternative detector configuration which eliminates the constraints of the others. In this configuration, each of the individual photodetectors is coupled to a 50 Ω line, and those lines are combined with a microwave signal combiner (0° hybrid). This combination eliminates the current modulation of one photodetector on the other, and consequently the intermodulation is lower than that of the configuration in Figure 3b. It has the advantage that it can be built with off the shelf microwave components coupled to conventional detectors. The disadvantage is that in combining power instead of current, the net detector gain is lower. This disadvantage, however, does not degrade the noise figure of the system if the individual detectors are each in the shot noise limit, as shown below.

Parallel Detectors

a) current summing



b) traveling wave



c) power summing

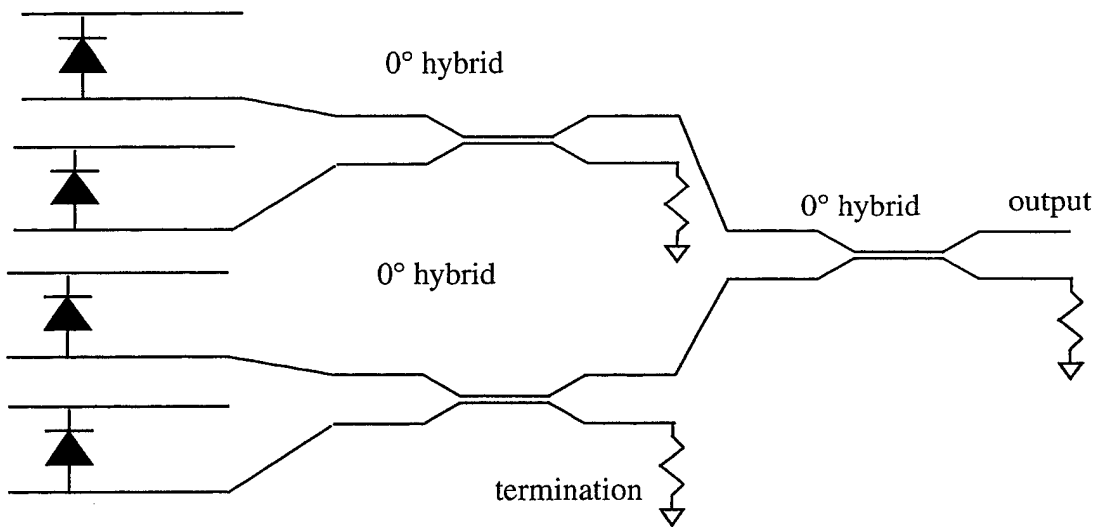


Figure 3. Detector structures for high power microwave signal detection

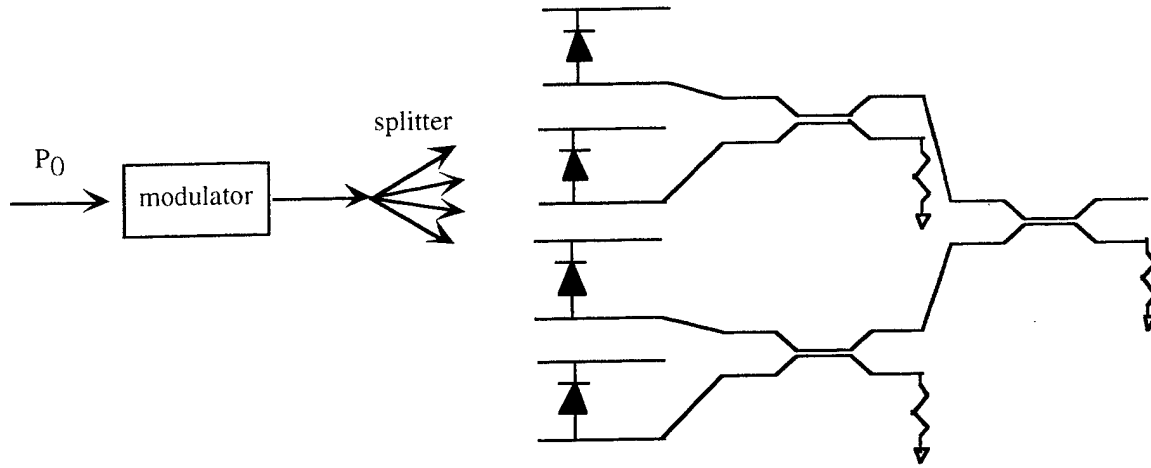


Figure 4. Link with detector from Figure 3c.

Figure 4 shows a generic external modulation direct detection link with the high power detector of Figure 3c. The input optical power, P_0 , is modulated by an intensity modulator with bias transmission T_0 and slope $\frac{dT}{dV}$. The output of the modulator is

$$P = P_0 \left(T_0 + V \frac{dT}{dV} \right) \quad (15)$$

This optical power is split into M photodetectors to generate the current at each photodetector

$$I_m = \frac{P_0}{M} \left(T_0 + V \frac{dT}{dV} \right) \mathfrak{R} \quad (16)$$

where \mathfrak{R} is the photodetector responsivity. The DC portion of this current generates the shot noise power $2 \frac{P_0}{M} T_0 \mathfrak{R} e B R$ where e is the electron charge, B is the bandwidth and R is the impedance of the line. The total noise on each photodetector is thus

$$N_m = 2 \frac{P_0 T_0 \mathfrak{R}}{M} e B R + k T B + \left(\frac{P_0 T_0 \mathfrak{R}}{M} \right)^2 t_i B R + \frac{P_0^2 \mathfrak{R}^2}{M^2} k T B R_m \left(\frac{dT}{dV} \right)^2 R \quad (17)$$

where k is Boltzmann's constant, T is the temperature, t_i is the laser RIN coefficient and R_m is the modulator input impedance. The first term is shot noise, the second is output thermal noise, the third term is the laser RIN noise, and the fourth is the input thermal noise on the modulator transmitted to the photodetector by the link.

The thermal noise and shot noise at each of these detectors is uncorrelated. The RIN and amplified input thermal noise at each detector is correlated. The microwave summing structure adds the power of the correlated signals at the 0° ports of the output and the

uncorrelated signals are passed half to each of the two outputs in each four port microwave hybrid. Consequently, the correlated signals have gain of M at the output giving us the total output noise power

$$N = 2 \frac{P_0 T_0 \mathfrak{R}}{M} eBR_{out} + kTB + (P_0 T_0 \mathfrak{R})^2 \frac{\tau_i BR_{out}}{M} + \frac{P_0^2 \mathfrak{R}^2}{M} kTBR_{in} \left(\frac{dT}{dV} \right)^2 R_{out} \quad (18)$$

where the right hand side terms correspond to shot, output thermal noise, RIN, and input thermal noise respectively.

The signal power at each photodetector is $\left(\frac{P_0}{M} V \frac{dT}{dV} \mathfrak{R} \right)^2 R_{out}$ and these powers are added coherently in the microwave hybrids to yield the output signal power

$$S = \frac{1}{M} P_0^2 \mathfrak{R}^2 V^2 \left(\frac{dT}{dV} \right)^2 R_{out} \quad (19)$$

Examination of equations (18) and (19) show that there is only one term which does not fall inversely with the number of detectors M . That is the second term in (18) the output thermal noise. If any of the other noise terms dominate output thermal noise by a reasonable margin, we can increase M without reducing the signal to noise ratio. The optical power level at which this occurs can be computed by comparing the first and second terms of equation (18). When the shot noise exceeds the thermal noise at each photodetector the division of the current into M channels gives us little noise penalty. The condition of being shot noise dominated occurs when

$$\begin{aligned} 2 \frac{P_0 T_0 \mathfrak{R}}{M} eBR_{out} &> kTB \\ \frac{P_0 T_0 \mathfrak{R}}{M} &> \frac{kT}{2eR_{out}} \end{aligned} \quad (20)$$

For a 50Ω load this occurs when the bias current from each photodetector, $P_0 T_0 \mathfrak{R}/M$, is more than 0.26 milliAmps. This very moderate current is compatible with all the high speed photodetectors and consequently if the microwave hybrid technique is cheaper to implement than the current summing techniques, no further investigation into high power photodetectors is necessary.

For RF link applications, noise figure is the key figure of merit. The noise figure is not degraded by low power detectors since combining the signals as shown above preserves the same output SNR. Consequently, RF photonic links are not limited by the photodetector because we can always add more power handling capability with the above

technique. This not only justifies our assumptions in other sections that the systems are not photodetector power limited, but this also should have impact on the current directions in photodetector research.

Task 2.2.2 Modulators

A great deal of effort is currently being invested in the development of modulators for RF photonics. Most emphasis of current work is for the application of point-to-point links. When these components are used in more powerful RF photonic systems, the trade-offs of optical power handling, single tone RF dynamic range (1 dB compression point), modulation depth and slope efficiency must be reevaluated. The requirements on the modulator are influenced by the system architecture. The utilization of summation before optoelectronic conversion of signals and the partitioning of the array into electronically steered sub arrays coupled with the signal environment affect the dynamic range required.

Efforts in high-power, highly-linear modulators have shown no breakthroughs in the recent years of intense research. LiNbO₃ modulators have had improvement in drive voltage and bandwidth, but further improvement is limited by RF loss on the microwave lines. Alternative modulators have finite power handling limitations or higher drive voltages.

The impact of coherent fan in gain on externally modulated RF photonic systems comes into play in relaxing preamplifier gain requirements for systems limited by moderate drive voltage modulators and increased dynamic range for systems with low noise figure.

Where the system goes into the low noise figure regime is also dependent on whether we use coherent versus incoherent summation. For low noise lasers, the systems become low noise figure when the last term in equations (8) and (12) are larger than the first terms, i.e. they are input thermal noise limited. For the incoherent and coherent systems this situation occurs for

$$\sqrt{N}V_{\pi} < \sqrt{\frac{\pi^2 kTB}{4eB} \mathcal{R}P_0 R_{in}} \quad (21)$$

For a 50Ω input, 1 Watt of total optical power, and 0.7 Amps/Watts detector responsivity, equation (21) indicates that the voltage must be 1.49Volts/ \sqrt{N} . For large N this requirement is out of reach and we must use a preamplifier in front of each modulator to lower the effective V_{π} .

Task 2.2.3 Light Sources

High power, low RIN light sources are a mature technology. However, the use of coherent systems prevents the use of multiple independent sources for each RF photonic link. The trade-off with coherent versus incoherent systems is the use of a single more powerful more expensive source versus a multitude of slightly less expensive sources. The demands on the light source power are ameliorated by the recovery of the available point to point gain with the fan-in gain inherent to coherent systems.

The occurrence of the summation over time delays in equation (9) of our analysis means that the laser itself may have RIN noise somewhat above that determined by the shot noise limit and the noise in not enter into the output. This unanticipated result favors the single high power laser over the multitude of independent sources since these lasers can be had with low RIN noise in the first place. The cost per unit power of these lasers is comparable to the cost of diode lasers and the phase noise is much smaller in diode pumped solid state lasers.

2.3 Task 3 Optimum Subarray Partitioning

The high current cost of RF photonic links has pushed a number of researchers to look towards electronically phase-only steered subarrays coupled to true-time-delay RF photonic links. One way to partition the problem is to provide just enough true-time-delay links to prevent appreciable beam squint. This occurs when the total delay across the subarray at the largest angle of incidence is less than the reciprocal bandwidth $N_{subarray} a \sin(\theta_{max})/c < 1/B$. This is the appropriate partition if the true-time-delay units are very expensive relative to the phase-only units and the cost of the true-time-delay units is independent of their dynamic range specifications.

At the onset of this contract we had evidence that the dynamic range required of a true-time-delay unit depends on the number of units utilized and the signal and interference scenario. The argument says that a subarray synthesizes an antenna function with gain and selectivity proportional to the size of the subarray. With a source of interference in proximity to the signal of interest, the modest selectivity of the subarray may not be enough to give higher gain to the signal of interest compared to the gain of the interference source. Because the subarray cannot achieve high suppression of interference sources, the gain of the subarray is given to the interference requiring that the photonic true-time-delay link must transmit this relatively high amplitude signal without distorting the signal of interest. Thus a large subarray size puts further demands on the dynamic range of the true-time-delay links. The conclusion of this argument is that if the cost of the true-time-delay link

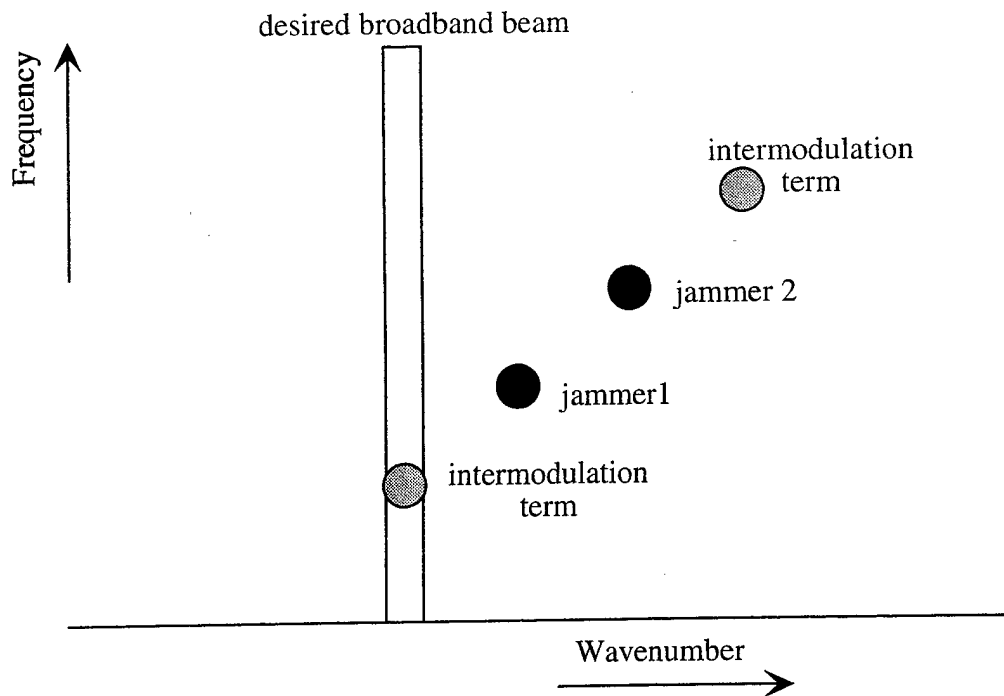


Figure 5. Frequency-wavenumber space representation of the received signals.

grows with the subarray size due to increased dynamic range requirements, it might be preferable to utilize more true-time-delay links (and hence smaller subarray size) than the squint based analysis requires, since each true-time-delay link has lower dynamic range requirements and thus is less expensive than in the large subarray case.

The above argument misses the gain of the intermodulation products caused by jammers out of the main beam whose wave-number mixes into the main beam. The argument is valid when considering dynamic range due to intermodulation products generated by nonlinear components which are downstream of the beamformer. However when the nonlinearity under consideration is that of the optical modulator it is upstream in the system, and the way it contributes to dynamic range limiting performance is shown below.

Figure 5 shows the frequency-wavenumber representation of the incoming signals on the array. The vertical axis is frequency and the horizontal axis is wavenumber, or angle of arrival. The signal of interest is a broad band signal at particular angle of arrival. Two jammers at particular angles of arrival, K_1 and K_2 and frequencies Ω_1 and Ω_2 are shown. The true time delay beam forming system maps all inputs at the angle of arrival of interest onto the output of the system. This beamforming operation reduces the power of the

jammers at other angles of arrival by the off axis beam rejection ratio. These jammers have reduced power at the system output and any nonlinear component there would be less taxed than had these jammers hit it full force. However the nonlinearities in the beam forming system mix the jammers to produce a two-tone third-order intermodulation product with frequency $2\Omega_2 - \Omega_1$ and wavenumber $2K_2 - K_1$. As shown in Figure 5, this intermodulation product may fall on the desired beam angle, and it is present regardless of the rejection of the high power jammers.

2.4 Task A DTIC Search

Note, this task was added in contract negotiations.

We searched the DTIC database for work relevant to this effort. We examined close to 100 abstracts generated by our key word search. Of these we ordered the full reports indicated in the following table. None of these reports duplicate the work contained herein.

AD Number	Title	Author
ADA239672	An Adaptive Coherent Optical Receiver Array.	Mercer, L. B.
ADA244402	Optoelectronics for Optically Controlled Phased-Array Systems.	Lau, Kam Y.
ADA257894	New Techniques in Optical Communications and Signal Processing.	Das, Pankaj K.; Stark, Henry; Vlannes, Nickolas P.
ADA260474	Novel Optical Processor for Phased Array Antenna.	Yao, Shi-Kay
ADA261983	Modified Acousto-Optic Adaptive Processor (Mod-AOAP).	Keefer, Christopher W.; Malowicki, John E.; Payson, Paul M.
ADA267056	System Architecture of Optically Controlled Phased Array Radar.	Lau, K. Y.
ADA267663	True Time Delay Optically Controlled Dual Band Transmitter.	Thai, Serey
ADA310906	Anti-Jamming Optical Beam Nuller.	Turbyfill, Michael E.; Lutsko, Jeffrey M.

ADA318134 Photonic True Time Delay Beamformer for a 20 Element L-Band Phased Array, Payson, Paul M.; Malowicki, John E.; Klumpe, Herbert W., III; Toughlian, Edward N.; Zmuda, Henry

3.0 References

- [1] Optoelectronic Signal Processing for Phased-Array Antennas IV, B.M. Hendrickson, SPIE, Los Angeles, January 1994.
- [2] L.B. Lambert, M. Arm, and A. Aimette, "Electro-optical signal processing for phased-array antennas," in *Optical and electro-optic information processing*, J. Tippett, Ed. MIT press, 1965.
- [3] Goutzoulis, A., Davies, K., and Johnson, A., "Development and field demonstration of a hardware-compressive fiber-optic true-time-delay steering system for phased-array antennas," *Applied Optics*, vol. 33, no. 35, pp. 8173-8185, Dec. 10, 1994.
- [4] R.T. Weverka and K. Wagner, "Adaptive phased-array radar processing using photorefractive crystals," in *Optoelectronic Signal Processing for Phased-Array Antennas II*, vol. 1217, B.M. Hendrickson and G. A. Koepf ed., *Proc. of the SPIE*, January , pp. 173-182, 1990.
- [5] Robert T. Weverka , Kelvin Wagner, and Anthony W. Sarto, "Optical processing for self-cohering of phased-array imaging signals", *Proceedings of SPIE Vol. 1703*, pp 552-565 1992
- [6] Robert T. Weverka, Kelvin Wagner and Anthony Sarto, "Adaptive phased-array radar processing using photorefractive crystals", *Applied Optics Vol. 35, No. 8*, Mar. 10, 1996, pp. 1344-1366